The Requirement for Carotenoids in the Assembly and Function of the Photosynthetic Complexes in *Chlamydomonas reinhardtii*[1][C][W][OA]

Stefano Santabarbara*, Anna Paola Casazza, Kulsam Ali, Chloe K. Economou, Thanyanun Wannathong, Francesca Zito, Kevin E. Redding, Fabrice Rappaport, and Saul Purton

Institute of Structural and Molecular Biology, University College London, London WC1E 6BT, United Kingdom (S.S., K.A., C.K.E., T.W., S.P.); Istituto di Biofisica (S.S.) and Insituto di Biologia e Biotecnologia Agraria (A.P.C.), Consiglio Nazionale delle Ricerche, 20133 Milan, Italy; Unité Mixte de Recherche 7099 Centre National de la Recherche Scientifique/Université Paris-7 (F.Z.) and Unité Mixte de Recherche 7141 Centre National de la Recherche Scientifique/Université Paris-6 (S.S., F.R.), Institut Biologie Physico-Chimique, F–75005 Paris, France; and Department of Chemistry and Biochemistry, Arizona State University, Tempe, Arizona 85287 (K.E.R.)

We have investigated the importance of carotenoids on the accumulation and function of the photosynthetic apparatus using a mutant of the green alga *Chlamydomonas reinhardtii* lacking carotenoids. The FN68 mutant is deficient in phytoene synthase, the first enzyme of the carotenoid biosynthesis pathway, and therefore is unable to synthesize any carotenes and xanthophylls. We find that FN68 is unable to accumulate the light-harvesting complexes associated with both photosystems as well as the RC subunits of photosystem II. The accumulation of the cytochrome b_6f complex is also strongly reduced to a level approximately 10% that of the wild type. However, the residual fraction of assembled cytochrome b_6f complexes exhibits single-turnover electron transfer kinetics comparable to those observed in the wild-type strain. Surprisingly, photosystem I is assembled to significant levels in the absence of carotenoids in FN68 and possesses functional properties that are very similar to those of the wild-type complex.

Carotenoids (Cars) are fundamental components of the photosynthetic apparatus (Young and Britton, 1993, and refs. therein). The vast majority of Cars are noncovalently bound to either the core or the antenna subunits of PSI or PSII (Siefermann-Harms, 1985; Bassi et al., 1993). The most abundant Car bound to the core subunits of both photosystems is β-carotene, which is found in the vast majority of oxygenic organisms (Siefermann-Harms, 1985; Bassi et al., 1993). The light-harvesting complexes (LHCs) that act as the outer antenna in plants and green algae bind a wider range of oxygenated Cars, known as xanthophylls, the most abundant of which is lutein (Siefermann-Harms, 1985; Bassi et al., 1993; Jennings et al., 1996). The stoichiometry of xanthophylls binding to LHC complexes depends on the particular complexes and often on the illumination conditions during the organism's growth (Siefermann-Harms, 1985; Demmig-Adams, 1990; Horton et al., 1996). Intriguingly, a molecule of β-carotene (as well as a molecule of chlorophyll [Chl] *a*) is found also in the cytochrome (Cyt) b_6f complex (Kurisu et al., 2003; Stroebel et al., 2003).

Cars have multiple functions in the photosynthetic process; they act as light-harvesting pigments (Frank and Cogdell, 1993), enlarging the optical cross section to radiation that is poorly absorbed by Chl. Moreover, Cars play a crucial role in processes such as nonphotochemical quenching that control the efficiency of light harvesting in response to the intensity of the incident radiation (for review, see Demmig-Adams, 1990; Horton et al., 1996; Niyogi, 1999). Probably the most important role of Cars in photosynthesis is the quenching of the excited triplet state of Chl (for review, see Frank and Cogdell, 1993; Giacometti et al., 2007), preventing the formation of highly reactive singlet oxygen, which represents the principal species active under high light stress (Hideg et al., 1994; Krieger-Liszkay, 2005). The importance of Cars is demonstrated by the observation that disruption of their biosynthesis through mutation, or by inhibition of a key enzyme in

[1] This work was supported by the Biotechnology and Biological Sciences Research Council (grant no. CO0350 and a studentship to K.A.), by a Royal Thai Government Scholarship (to T.W.), and by the U.S. Department of Energy (grant no. DE–FG02–08ER15989 to K.E.R.).

* Corresponding author; e-mail stefano.santabarbara@cnr.it.

The authors responsible for distribution of materials integral to the findings presented in this article in accordance with the policy described in the Instructions for Authors (www.plantphysiol.org) are: Stefano Santabarbara (stefano.santabarbara@cnr.it) and Saul Purton (s.purton@ucl.ac.uk).

[C] Some figures in this article are displayed in color online but in black and white in the print edition.

[W] The online version of this article contains Web-only data.

[OA] Open Access articles can be viewed online without a subscription.

www.plantphysiol.org/cgi/doi/10.1104/pp.112.205260

the pathway, leads to either lethal phenotypes or to rapid photobleaching of the photosynthetic tissue (Claes, 1957; Faludi-Dániel et al., 1968, 1970; Bolychevtseva et al., 1995; Trebst and Depka, 1997).

Moreover, it has been shown that the presence of xanthophylls is absolutely necessary for refolding in vitro of LHC I and LHC II antenna complexes (Plumley and Schmidt, 1987; Paulsen et al., 1993; Sandonà et al., 1998). Such Cars, therefore, have a structural role, as well as their involvement in light harvesting, nonphotochemical quenching regulation, and the quenching of the Chl triplet state. Whether Cars also play a key structural role in the formation and stability of the core complexes of both PSI and PSII has not been systematically explored, since assembly of these complexes in vitro is not feasible. Studies in vivo using higher plants are complicated by the fact that Car deficiency is lethal and can be studied only during the early stages of greening and leaf development (Faludi-Dániel et al., 1968, 1970; Inwood et al., 2008). In these studies, it was shown that the accumulation of PSII complexes was greatly impaired in mutants of maize (*Zea mays*; Faludi-Dániel et al., 1968, 1970; Inwood et al., 2008), while the assembly of PSI appeared to be less sensitive to Car availability. In mutants of the cyanobacterium *Synechocystis* sp. PCC 6803 lacking the genes for phytoene desaturase or ζ-carotene desaturase, there was a complete loss of PSII assembly, while functional PSI complexes were assembled, albeit with slightly altered electron transfer kinetics with respect to the wild-type complex (Bautista et al., 2005). In agreement with the higher sensitivity of PSII assembly to Car availability, Trebst and Depka (1997) reported a specific effect on the synthesis of the D1 subunit of PSII RC upon treatment with phytoene desaturase inhibitors. On the other hand, it has recently been reported that in lycopene-β-cyclase mutants of Arabidopsis (*Arabidopsis thaliana*) that have a decreased amount of β-carotene (bound to the RC) with respect to most of the xanthophyll pool pigments (bound to the LHCs), the level of accumulation of PSI complexes, particularly that of the LHC I complement, was more affected that that of PSII, probably also because of an increased sensitivity to photodamage of mutated PSI RC (Cazzaniga et al., 2012; Fiore et al., 2012).

In this investigation, we have studied the accumulation and functionality of the major chromophore-binding complexes of the photosynthetic apparatus, PSI, PSII, and Cyt b_6f, in a Car-less mutant of the green alga *Chlamydomonas reinhardtii* (FN68) that is blocked at the first committed step of Car biosynthesis, namely, phytoene synthesis (McCarthy et al., 2004). Although the mutant is incapable of growing under phototrophic or photomixotrophic conditions, it can grow in complete darkness on a medium supplemented with a carbon source. Here, we show that the PSII core and antenna complexes fail to accumulate in the mutant and that the Cyt b_6f complex accumulates to approximately one-tenth of the wild-type level. On the other hand, the PSI reaction center accumulates in FN68 and possesses electron transfer properties that are remarkably similar to those of wild-type PSI. Interestingly, we find that the level of PSI accumulation differs in other phytoene synthase null mutants, suggesting that additional mutations in one or other of these strains affect PSI stability. Nevertheless, our findings demonstrate that Cars are not required for either the assembly or the functionality of PSI in vivo.

RESULTS AND DISCUSSION

The Car Deficiency and Light Sensitivity of FN68 Are Due to a Lesion in the Phytoene Synthase Gene

The FN68 mutant of *C. reinhardtii* was isolated in the 1970s as an extremely light-sensitive strain blocked in the biosynthesis of phytoene, the first product of the Car biosynthetic pathway (Foster et al., 1984). FN68 has been described as a "colorless" or "white" mutant (Foster et al., 1984; McCarthy et al., 2004), although the strain is in fact pale green due to the presence of Chl *a* (Fig. 1). Our pigment analysis has confirmed that FN68 lacks any detectable phytoene or other Cars and has only trace (less than 2%) amounts of Chl *b*, but it accumulates approximately 20% of wild-type Chl *a* levels, (Supplemental Fig. S1). This value is comparable with the approximately 16% Chl *a* reported by McCarthy et al. (2004), although the precise amount of Chl *a* in FN68 appears to be dependent on cell age (data not shown). A molecular analysis of FN68 and other Car-less mutants of *C. reinhardtii* by McCarthy et al. (2004) revealed that all these mutants carry point mutations in the nuclear gene (*PSY*) encoding phytoene synthase. In the case of FN68, the lesion is a frame-shift mutation in exon 2, which also results in the loss of an *Sph*I restriction site (Supplemental Fig. S2). In order to confirm that this mutation was exclusively responsible for the observed phenotype, we transformed FN68 with a 4.4-kb PCR-amplified genomic fragment containing the wild-type *PSY*. Transformants were selected based on their ability to form colonies in the light. As shown in Figure 1, the FN68::*PSY* transformants have restored pigmentation, are insensitive to light, and are capable of phototrophic growth (although phototrophic growth overall is slower than in the wild type, probably as a

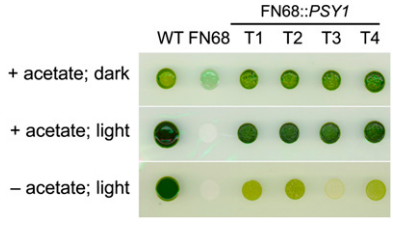

Figure 1. Growth phenotypes on solid medium of the wild type (WT), FN68, and FN68 transformed with wild-type *PSY* (T1–T4). Colonies were grown under heterotrophic (acetate, no light), mixotrophic (acetate, light), and phototrophic (no acetate, light) conditions. [See online article for color version of this figure.]

result of unrelated secondary mutations acquired by FN68 over 40 years of maintenance of the strain in the dark). The presence of the introduced wild-type *PSY* allele, along with the original mutant allele, in each transformant line was confirmed by molecular analysis using the *Sph*I polymorphism as a marker (Supplemental Fig. S2).

Cars Are Required for the Accumulation of PSII and LHCs But Not PSI

Figure 2 shows the absorption spectra of whole cells of *C. reinhardtii* recorded at room temperature (Fig. 2A) and the fluorescence emission spectra recorded at 77 K (Fig. 2B). Spectra from FN68 are compared with those of the wild type and also the mutant Fud7-P71, which lacks PSII and most of the LHC complement but harbors wild-type amounts of PSI (Byrdin et al., 2006). The absorption spectrum of the wild-type strain displays a pronounced shoulder at 645 nm, arising from absorption of Chl *b* present in the LHCs, whereas this feature is absent in the Fud7-P71 and FN68 spectra. The contribution of carotene, and of Chl *b*, to the wild-type spectrum is seen as a strong absorption between 450 and 500 nm. Again, this feature is absent in the FN68 spectrum and is reduced in the Fud7-P71 mutant, where only PSI Cars are present. The fluorescence emission spectrum from the wild type shows the characteristic peaks, at 685, 695, and 715 nm, that are assigned to PSII (685/695 nm) and PSI (715 nm); a shoulder is also observed at 682 nm and reflects the preequilibrated emission from LHC II (Butler, 1978; Rijgersberg and Amesz, 1980). FN68 lacks the PSII signals but shows a principal broad band at 715 nm arising from functional PSI, indicating that, at least at low temperature, energy transfer within the Chl *a* bound to the PSI core antenna complexes is not perturbed to any significant extent. The Fud7-P71 spectrum is very similar to that of FN68 at wavelengths longer than 690 nm, but the former shows a clear peak at 682 nm, which arises from the residual fraction of antenna, most likely disconnected from the reaction centers, present in this strain.

Figure 2C shows the separation of photosynthetic complexes on a nondenaturing gel following solubilization of thylakoid membranes with the mild detergent β-*n*-dodecyl maltoside. In the case of wild-type membranes, three main bands can be resolved on the gel, and these are assigned as nondissociated PSI/PSII supercomplexes, the PSI-LHC I supercomplex, and the monomeric LHC complexes (Supplemental Fig. S3). In the FN68 mutant, only a single band is observed on the nondenaturing gel, which migrates slightly below the PSI-LHC I supercomplex and which is assigned to the PSI core complex. This indicates that both the PSII core and the LHC I and LHC II complexes accumulate to a

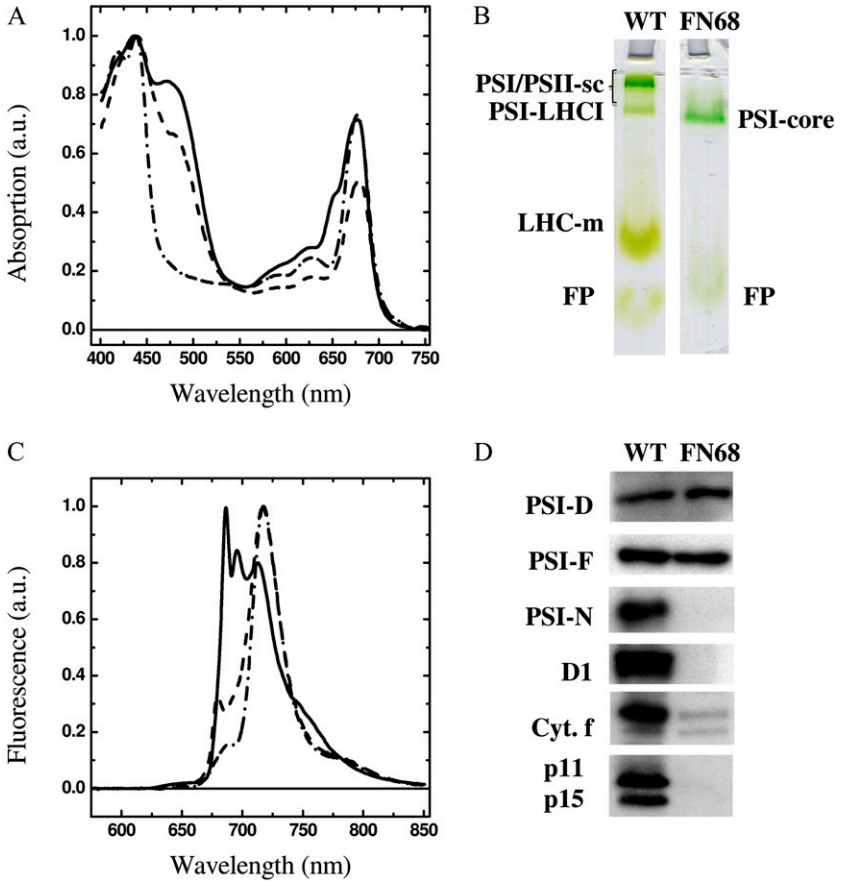

Figure 2. A and B, Absorption spectra of whole cells of *C. reinhardtii* at room temperature (A) and fluorescence emission spectrum at 77 K upon excitation at 460 nm (B). Solid lines, the wild type; dashed lines, Fud7-P71 strain; dashed-dotted lines, FN68. The spectra are normalized to maximal absorption and fluorescence emission, respectively. a.u., Arbitrary units. C, Deriphat-PAGE of thylakoid membranes (35,000*g* fractions) from the wild type (WT) and FN68. PSI/PSII-sc, Nondissociated PSI/PSII supercomplexes; LHC-m, monomeric LHC; FP, free pigment. Lanes were loaded based on equal Chl (5 μg Chl *a*+*b*) concentration. D, Immunoblot analysis of whole cell extracts using antibodies raised to subunits of PSI (PsaD, PsaF, PsaN), PSII (D1), Cyt b_6f complex (Cyt. *f*), and LHC of PSI (p11) and of PSII (p15). Lanes were loaded based on equal cell numbers. [See online article for color version of this figure.]

level that is below the detection sensitivity of the technique (Fig. 2C). Moreover, the lack of PSII, as well as the LHC complement in FN68, is confirmed by western-blot analysis, using antibodies directed against the PSII core protein D1 and outer antenna complexes of PSII and PSI, respectively (Fig. 2D). In contrast, the accumulation of two of the core PSI subunits (PsaD and PsaF) is seen in FN68, indicating PSI accumulation in the mutant (Fig. 2D). This level of PSI was judged to be approximately 25% of the wild type, as shown in Supplemental Figure S4, although the actual level appears to vary depending on cell age (data not shown). The absence of Cars, therefore, appears not to prevent the stable accumulation of PSI, a complex that contains approximately 22 β-carotene molecules (Jordan et al., 2001; Ben-Shem et al., 2003). Their absence, however, does result in a failure to accumulate the PsaN subunit. This peripheral subunit is bound by weak electrostatic interactions to the lumenal face of PSI, and PsaN does not bind any of the β-carotenes itself (Ihalainen et al., 2002). It is most likely that either structural distortions at the lumenal face are responsible for a failure of PsaN binding, leading to the degradation of the unassembled subunit, or the nucleus-encoded subunit is not imported correctly into the thylakoid membranes, and therefore is degraded, since this process is ΔpH (for change in pH) dependent (Nielsen et al., 1994) and photosynthetic electron transfer (ET) is severely impaired in FN68. In both cases, the steady-state level of PsaN will fall below the level of detection.

In contrast to PSI, the stable accumulation of the PSII complex appears to be dependent on one or more of the 12 β-carotene molecules present in the core of PSII (Guskov et al., 2009; Umena et al., 2011). The failure of PSII accumulation in Car-deficient mutants, or in plant seedlings treated with the Car inhibitor norflurazon, has been noted previously (Trebst and Depka, 1997; Humbeck et al., 1989; Bolychevtseva et al., 1995; Bautista et al., 2005; Inwood et al., 2008). Similarly, the absence of carotenes severely impairs the accumulation of both LHC I and LHC II, which substantiates the results obtained in vitro and points toward a crucial structural role of xanthophylls in promoting and/or stabilizing the folding of these complexes (Plumley and Schmidt, 1987; Sandonà et al., 1998).

Rescue of FN68 by transformation with wild-type *PSY* results in the restoration of wild-type levels of both PsaN and D1 as well as the LHC complement for both PSII and PSI, confirming that it is the absence of Cars that is the cause of the observed destabilization effects and the resulting accelerated degradation of the unassembled subunits (Supplemental Fig. S5).

Stable Accumulation of the Cyt b_6f Complex Is Affected by Loss of the Single β-Carotene Molecule

The Cyt b_6f complex contains a single Car molecule of unknown function (Kurisu et al., 2003; Stroebel et al., 2003). As shown in Figure 2D, the loss of this Car has a significant effect on the steady-state level of the complex, as judged by the accumulation of the Cyt *f* subunit in FN68. The level of Cyt b_6f was investigated further by comparing the accumulation of other subunits in the mutant with the wild type: a Cyt b_6f mutant lacking subunit IV (Δ*petD*) and the Fud7-P71 strain using antibodies directed against Cyt *f*, Cyt b_6, and subunit IV (Fig. 3A). In addition, parallel gels were stained with the heme stain 3,3′,5,5′-tetramethylbenzidine to reveal the Cyt-binding subunits of the complex (Fig. 3B). As observed for the Cyt *f* subunit, the other subunits show only a low level of accumulation (below 15%), although the actual amount was found to be variable between different cell preparations (e.g. compare FN68 Cyt *f* levels in Fig. 3 with those in Supplemental Fig. S5). It is likely that this reflects differences in the growth phase of the FN68 cultures, since it has been shown that Cyt b_6f levels decrease significantly in other mutants affected in the complex once cells start to enter stationary phase (Choquet and Vallon, 2000).

The Car-Minus Cyt b_6f Complex in FN68 Is Functional

We investigated whether the loss of the Car molecule affected the functionality of the remaining Cyt b_6f

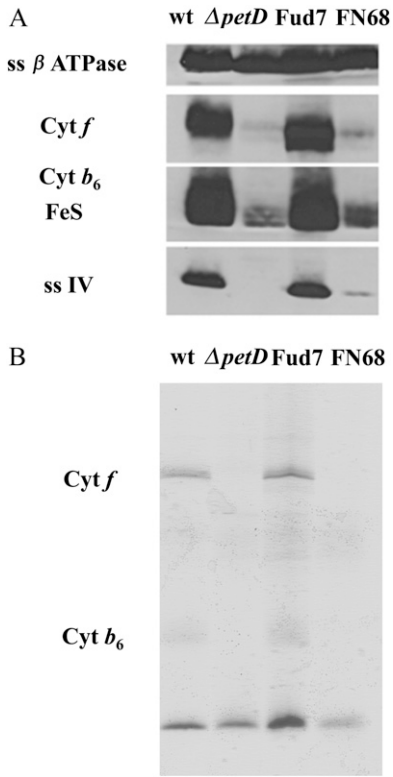

Figure 3. Biochemical characterization of the Cyt b_6f complex in the FN68 mutant. Immunoblot (A) and specific heme staining for Cyt *f* and Cyt *b* (B) are shown for membrane protein extracts probed with antibodies against Cyt *f*, Cyt b_6, subunit IV, the Rieske iron-sulfur center (FeS), and subunit β of the ATP synthase. Loading was normalized based on an equal Chl basis. wt, Wild type.

by monitoring the turnover of the complex in response to a single, saturating, turnover flash. Cyt *f* is mainly reduced under dark, microaerobic conditions. Consequently, the kinetics of Cyt *f* oxidation by plastocyanin can be monitored spectroscopically following actinic laser-flash excitation of PSI. FN68 was compared with the Fud7-P71 strain, which contains a wild-type amount of both PSI and Cyt b_6f complexes. Measurements were performed in this strain, because the absence of the PSII core subunit and the low antenna contents greatly reduce background absorption, resulting in a large increase in the signal-to-noise ratio, and also allows measurements in the near UV using whole cells (Guergova-Kuras et al., 2001; Byrdin et al., 2006). Moreover, apart from the accumulation of Cyt b_6f and the residual presence of a small fraction of LHCs, its thylakoid composition closely matches that observed in FN68.

In Figure 4, A and B, the kinetics recorded at several wavelengths in the region of maximal absorption of the more diagnostic Cyt α and the β-bands are shown. Optical transients were analyzed by a global fitting routine (400–600 nm) to extract the decay time constants and decay-associated spectra (DAS), which are shown in Figure 4, C and D. The DAS are internally normalized by the maximal bleaching of the difference spectrum associated with the metastable electron donor P700 (P_{700}^{+}-P_{700}), which peaks at 430 nm.

In the control and the Car-deficient strains, three kinetic components were required to describe the kinetics following a single turnover flash. Two of these

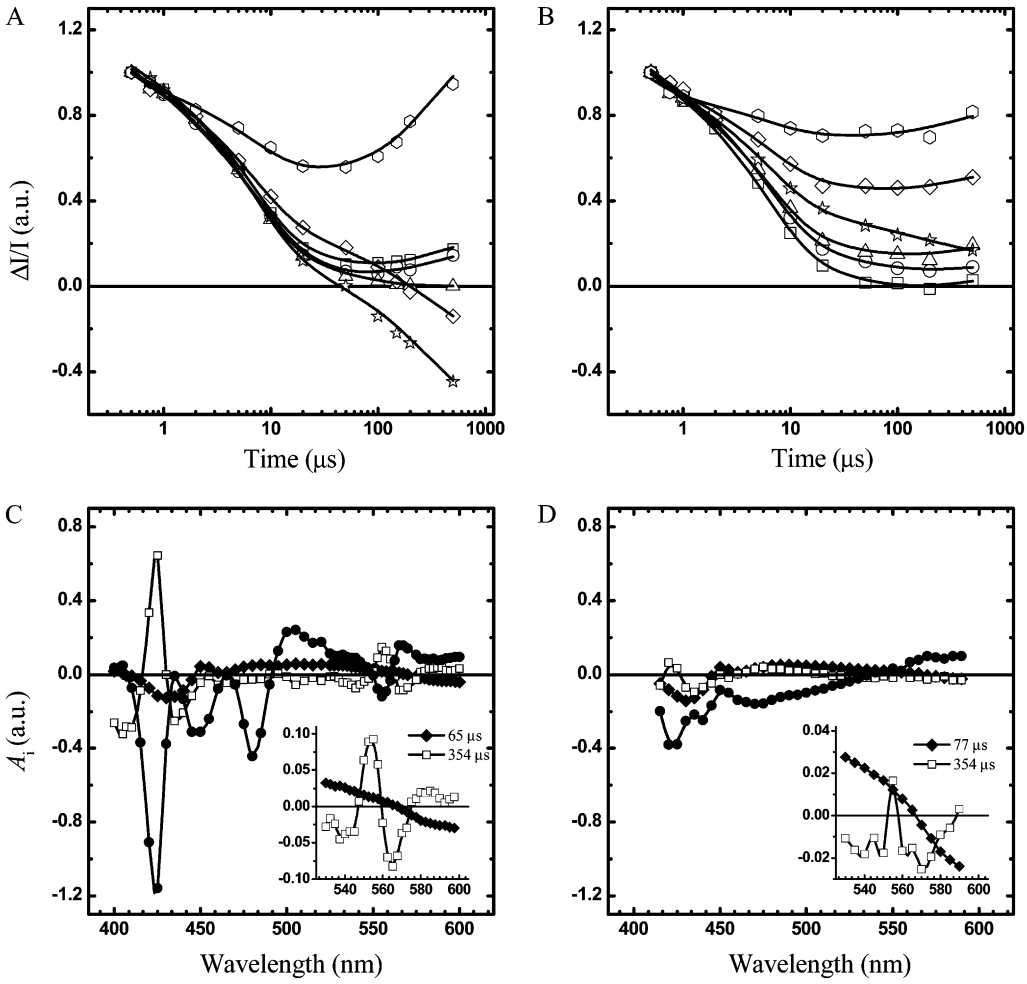

Figure 4. A and B, Kinetics of difference absorption induced by saturating laser excitation in whole cells of strains Fud7-P71 (A) and FN68 (B) at room temperature in the 0.5- to 100-μs time range. Detection wavelengths were as follows: 540 nm (squares), 545 nm (circles), 550 nm (triangles), 555 nm (stars), 560 nm (diamonds), and 565 nm (hexagons). Continuous lines are the fit to the experimental data with a sum of exponential function. Each kinetic trace is normalized to the intensity of the ΔI/I signal at 10-ns delay. C and D, DAS obtained from global fitting of the kinetic transient in the Fud7-P71 (C) and the FN68 (D) strains. For DAS, τ = 77 μs (black diamonds), τ = 357 μs (white squares), offset (black circles). The insets show the details of the DAS in the α- and β-bands of Cyt b_6f absorption for 77 and 357 μs. The DAS are normalized to the value of extrapolated P_{700}^{+} absorption bleaching at 430 nm, extrapolated to $t_{\rightarrow 0}$ (for time that tends to zero). a.u., Arbitrary units.

have virtually identical DAS and reflect the heterogeneous kinetics of P_{700}^+ reduction by plastocyanin (Fig. 4, C and D). Their associated lifetimes are 6.5 and 67 μs, in agreement with previous investigations of *C. reinhardtii* (Santabarbara et al., 2009; for review, see Haehnel, 1984). The slower component has a 354-μs lifetime, and its DAS is fully consistent with the oxidation of Cyt *f* (for review, see Hope 2000); it displays a maximum at approximately 554 nm, which is a characteristic feature of Cyt *f* (Fig. 4, C and D, insets), and a major positive peak at 425 nm in the Cyt γ band (Fig. 4, C and D). A nondecaying (i.e. lifetime [τ] $>$ 1 ms) component with large amplitude is also observed, which reflects, principally, the reduction of oxidized Cyt *f* and the oxidation of Cyt *b*. Although the lifetime of all three components developing in the hundreds of microseconds time scale is virtually the same in the FN68 and the Fud7-P71 strains, the DAS spectrum attributed to oxidation of Cyt *f* has an approximately 10-fold smaller amplitude in FN68, after normalization to P_{700}^+ bleaching. Thus, this characterization of Cyt b_6f catalytic activity following a single turnover flash indicates that the residual fraction of the complex in the FN68 strain is functional.

Table I. *Global fit parameters describing the kinetics of A_1^- oxidation and P_{700}^+ reduction at room temperature in vivo*

Global fitting analysis is shown for the optical transient in whole cells of Fud7-P71 and the FN68 mutant. The data have been fitted by the linear sum of exponential functions: $y(t) = \sum_{i=1}^{n} A_i(\lambda)e^{-t/\tau_i} + A_\infty(\lambda)$, where $A_\infty(\lambda)$ is a nondecaying component in the time range investigated. The fractional amplitude of the components in the nanosecond range [$f(A_\lambda)$] at three characteristic wavelengths is calculated as: $f(A_\lambda) = |A_{i,\lambda}| \times (\sum_{i=1}^{n} |A_{i,\lambda}|)^{-1}$.

Sample	Lifetime	$f(A_{390})$	$f(A_{430})$	$f(A_{480})$
	ns			
Fud7-P71 (control)				
τ_1	28.3	0.41	0.09	0.24
τ_2	286.4	0.58	0.06	0.26
τ_3	6754	0.01	0.85	0.51
FN68				
τ_1	28.4	0.26	0.04	0.14
τ_2	312.5	0.61	0.13	0.28
τ_3	6547	0.13	0.83	0.54

Electron Transfer Reactions in the PSI RC of FN68

In order to understand the role of bound Cars in the electron transfer properties of the PSI RC, we have measured the kinetics of the oxidation of the secondary electron acceptor, phylloquinone A_1, in whole cells and at room temperature. Laser-induced optical transients were acquired in the 360- to 570-nm interval (selected kinetics are shown in Supplemental Fig. S6) and globally fitted to extract time constants (Table I) and DAS (Fig. 5). The kinetic traces recorded in the FN68 and Fud7-P71 strains are globally described by three lifetime components. Two of these decays fall in the nanosecond time scale and have values of 24 and 258 ns in the Fud7-P71 strain and 22 and 316 ns in the FN68 mutant. Thus, while the apparent rate of the fast component of A_1^- oxidation, which is associated with the PsaB-bound phylloquinone (A_{1B}; Guergova-Kuras et al., 2001; Ali et al., 2006; Byrdin et al., 2006), has almost the same value in the FN68 and the control strain, the slow phase, which principally arises from the oxidation of the PsaA-bound A_{1A} quinone (Guergova-Kuras et al., 2001; Byrdin et al., 2006; Santabarbara et al., 2008, 2010c), is affected, although not in a dramatic fashion, by the absence of Cars in the complex.

The DAS of the two nanosecond components assigned to A_1^- oxidation show clear positive peaks at approximately 480 and 510 nm and negative peaks at approximately 500 nm in the control strain, which are attributed to electrochromism (ECS) of RC pigments in response to the field generated by the electron transfer reactions. In contrast, a single broad and asymmetric feature peaking at approximately 482 nm is observed in FN68. The absence of fine spectral structure at wavelengths longer than 465 nm in the DAS of both the 24- and 316-ns components is simply the result of the absence of Cars in the PSI RC of the FN68 mutant. At the same time, it highlights the fact that the electrochromic signal, in this wavelength interval, has an important, and at several wavelengths, dominant, contribution from Chl. An intense signal peaking at approximately 450 nm, which is observed in both the 24- and 316-ns DAS of FN68, can be attributed primarily to the electrochromic response of Chl(s) near the phylloquinone cofactors. This feature is more resolved in FN68 than in the control strain, probably due to the disappearance of overlapping ECS signals from Cars. Interestingly, as noted previously by Bautista et al. (2005) in Car-deficient mutants of *Synechocystis* sp. PCC 6803, the maximum bleaching is blue shifted by 5 nm in the 24-ns DAS (450 nm) with respect to the 316-ns DAS (455 nm). This difference can be interpreted in terms of a different local environment of the Chl(s) near A_{1A} and A_{1B}, providing further evidence of the assignment of these kinetic phases.

The DAS of the approximately 6-μs decay components reflects the reduction of P_{700}^+ by plastocyanin (PC). The P_{700}^+PC-P_{700}PC$^+$ difference spectra recorded in the control and FN68 strains are very similar at wavelengths lower than 460 nm. However, at longer wavelengths, clear differences are seen, which can also be attributed to the absence of Cars in the RC of FN68. The spectrum of P_{700}^+ reduction exhibits only a broad feature peaking at about 490 nm in FN68, whereas in Fud7-P71 RC, features originating from electrochromic shifts in Chls near P_{700} are observed at 485, 505, and 530 nm.

The results obtained in vivo in the FN68 strain of *C. reinhardtii* are qualitatively in excellent agreement with a previous investigation by Bautista et al. (2005), who

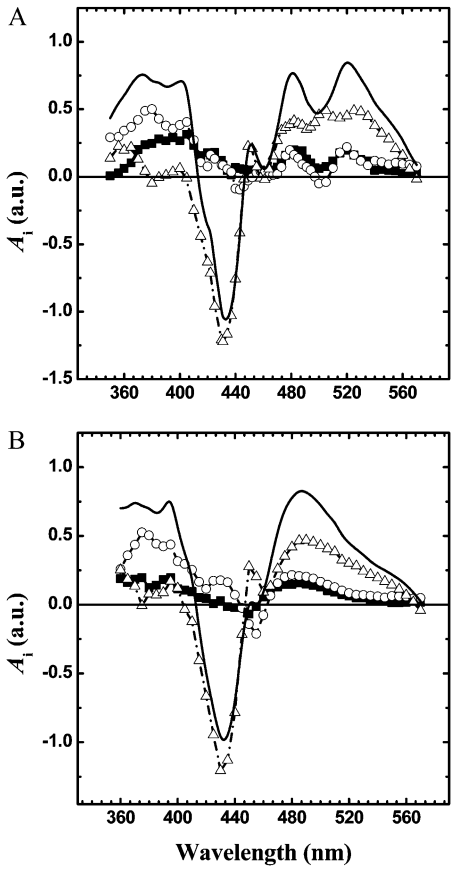

Figure 5. DAS obtained from global fitting of the kinetic transient in the near UV and visible regions of the absorption spectrum. Black squares/solid lines, 20-ns component; white circles/solid lines, 250-ns component; white triangles/dashed-dotted lines, 6-μs component (for precise values, see Table I). The continuous line is the initial spectrum calculated at $t_{\to 0}$ (for time that tends to zero) after subtraction of nondecaying signal within the sampled time window. The DAS are normalized to the value of the $t_{\to 0}$ spectrum at 430 nm. A, FuD7-P71 (control). B, FN68.

studied the effect of mutations at the level of phytoene desaturase and ζ-carotene desaturase on isolated PSI from *Synechocystis* sp. PCC 6803. Even though these mutations are downstream to phytoene synthase, they still result in strong depletion of Car from isolated PSI particles (Bautista et al., 2005). In PSI containing either only phytoene or ζ-carotene, it was shown that the lifetime of the rapid phase of A_1^- oxidation was substantially unaffected, but the slow component displayed a moderate lengthening (Bautista et al., 2005), as observed in whole cells of FN68 (Fig. 5). However, while the relative amplitudes of 20- and 250-ns DAS were substantially unaltered in the Car biosynthetic mutants of *Synechocystis* sp. PCC 6803 compared with the wild type, we observed a slight decrease in the relative contribution of the approximately 20-ns phase with respect to the 250-ns phase in the FN68 strain. Based on the kinetic measured at 390 nm (and the overall DAS in the 360- to 400-nm range), the amplitude ratio is shifted from 1:1.4 (20:250 ns) in the control strain RC to 1:2.3 in the FN68 Car-depleted complex (Table I). As a large perturbation of extinction coefficients associated with the absorption of either the semiquinone or quinone form of A_{1A} and A_{1B} appears unlikely (note that the total absorption difference with respect to P_{700}^+ is substantially unmodified in FN68 with respect to the control strain), the simpler rationalization for the small decrease in amplitude of the approximately 20-ns phase with respect to the approximately 250-ns phase is a subtle redistribution of the relative amount of electrons (statistically) transferred by the ET_A and ET_B redox chains in favor of the former. That such redistribution can indeed occur has been demonstrated in site-directed mutants affecting either the coordination of ET cofactors located upstream of A_1 (Byrdin et al., 2006; Li et al., 2006; Santabarbara et al., 2008) or altering the strength of hydrogen bonding to A_1 (Santabarbara et al., 2010c; Srinivasan et al., 2011).

Pulsed Electron Paramagnetic Resonance Analysis of the PSI RC in FN68 at 265 and 100 K

The kinetics of electron transfer in the PSI reaction center lacking carotenes was also investigated by time-resolved pulsed electron paramagnetic resonance (EPR), a technique complementary to transient absorption, which has also been extensively used to characterize the secondary/ternary ET reactions in PSI (Santabarbara et al., 2005a; Srinivasan and Golbeck 2009). When applied to laser-flash excitation, pulsed EPR has the advantage of being selective for spin-correlated radical pairs, such as $[P_{700}^+A_1^-]$, which is by far the dominating signal detected in thylakoid membranes (Santabarbara et al., 2005b, 2006, 2010b). Therefore, experiments can be performed in the wild-type background without loss of sensitivity. A summary of the comparative analysis of the kinetics of ET in PSI monitored by time-resolved electron spin echo (ESE) spectroscopy in the wild type and FN68 is presented in Table II (a more detailed discussion and the experimental data are presented in Supplemental Fig. S7).

The decay of the ESE monitored at 265 K (close to room temperature) provides information on $[P_{700}^+A_{1A}^-]$ only, since $[P_{700}^+A_{1B}^-]$ is not detected due to the temporal resolution of the spectrometer (approximately 50 ns). The analysis of time-resolved ESE experiments is in qualitative agreement with the results obtained by optical spectroscopy, indicating a slower oxidation of A_{1A}^- in FN68 compared with the wild type. However, the effect on the kinetics is more pronounced when monitored at 265 K than at room temperature, suggesting that the absence of carotene in PSI might influence the activation barrier of this reaction (see the discussion of Supplemental Fig. S6 for further details).

Moreover, we have studied the decay of ESE signal at 100 K. At this temperature, the ESE signal provides information concerning charge recombination reactions rather than forward ET (Schlodder et al., 1998; Agalarov and Brettel 2003; Santabarbara et al., 2005a,

Table II. *Fit parameters describing the decay of "out-of-phase" ESE*

Fit parameters are shown describing the decay of the ESE after the actinic laser flash in thylakoids isolated from the wild type and FN68 strain. Ascorbate (10 mM) with 200 μM phenazinemethosulfate as mediator was used to reduce P_{700}^+ in the experiments performed at 265 K. The other samples were dark adapted for 30 min in the presence of $Na_2S_2O_4$ (11 mM, pH 8; $F_{A/B}$ reduced, F_X oxidized). Preillumination of the sample for 5 min at 205 K results in full reduction of $F_{A/B}$ and more than 80% reduction of F_X ($F_{A/B/X}$ reduced). The decays were fitted to a sum of an exponential function, $y(t) = \alpha_1 e^{-t/\tau 1} + \alpha_2 e^{-t/\tau 2}$ and $\tau_{av} = \alpha_1 \times \tau_1 + \alpha_2 \times \tau_2$, with $\alpha_1 + \alpha_2 = 1$ (where α is the associated amplitude).

Sample	τ_1	α_1	τ_2	α_2	τ_{av}
	ns		*ns*		*ns*
Decay of the ESE at 265 K					
Wild Type	305 ± 4	0.93 ± 0.1	1,585 ± 48	0.07 ± 0.05	488 ± 5
FN68	226 ± 8	0.37 ± 0.5	964 ± 10	0.63 ± 0.8	693 ± 7
Decay of the ESE at 100 K, $F_{A/B}$ reduced, F_X oxidized					
Wild type	2.36 ± 0.4	0.11 ± 0. 08	22.2 ± 0.8	0.89 ± 0.08	20.0 ± 0.9
FN68	2.14 ± 0.6	0.09 ± 0.1	19.5 ± 0.4	0.91 ± 0.07	17.9 ± 0.7
Decay of the ESE at 100 K, $F_{A/B/X}$ reduced					
Wild type	2.13 ± 0.5	0.37 ± 0.06	18.9 ± 0.6	0.63 ± 0.02	12.7 ± 0.4
FN68	2.05 ± 0.5	0.29 ± 0.08	15.5 ± 0.8	0.71 ± 0.07	11.6 ± 0.6

2010b). Both in the wild type and in FN68, under conditions in which the successive electron acceptor iron-sulfur cluster (F_X) is initially oxidized, the signal is dominated by an approximately 20-μs lifetime that arises from [$P_{700}^+A_{1A}^-$] (Santabarbara et al., 2005b, 2006). Upon F_X prereduction, the decay becomes biphasic, and it is characterized by lifetimes of approximately 2 and 20 μs, both in the wild type and FN68. The approximately 2-μs phase was shown to arise from the [$P_{700}^+A_{1B}^-$] radical pair (Santabarbara et al., 2005b, 2006, 2010b). The need to reduce F_X to observe [$P_{700}^+A_{1B}^-$] was interpreted in terms of a difference in the driving forces for A_{1A}^- and A_{1B}^- oxidation, being thermodynamically unfavorable (i.e. the standard free energy difference > 0) for the former and favorable (standard free energy difference < 0) for the latter (Santabarbara et al., 2005a, 2010a). Such "functional asymmetry" in $A_{1A/B}$ energetic properties appears to be qualitatively conserved in FN68. This is also confirmed by the observation that PSI assembled in FN68 is capable of reducing the terminal acceptor iron-sulfur clusters $F_{A/B}$ at low temperature (Supplemental Fig. S8). Finally, the relative amplitudes of the approximately 2- and 20-μs phases (Table II) provide a measure of the statistical utilization of ET_B and ET_A (Santabarbara et al., 2005b, 2006, 2010b). The analysis of charge recombination reaction monitored by the ESE decay also shows a redistribution in favor of ET_A, although it is less pronounced than that observed at room temperature.

Stability and Functionality of the Electron Transfer Components in the Absence of Carotenes

As discussed above, the Cyt b_6f complex binds one β-carotene and one Chl *a* molecule as prosthetic groups in addition to cofactors active in electron transfer reactions (Kurisu et al., 2003; Stroebel et al., 2003). Spectroscopic investigations (Peterman et al., 1998; Dashdorj et al., 2005) of the bound chromophores indicate that the β-carotene molecule does not directly interact with the Chl *a*. Thus, the β-carotene bound to Cyt b_6f should be incapable of directly quenching the Chl triplet state. The function of these two pigment molecules within the complex are at present unknown, although it has been suggested that β-carotene might play a photoprotective role by directly scavenging singlet oxygen (Dashdorj et al., 2005). It has also been proposed that the β-carotene might play a structural role, acting as a lipid analog and stabilizing the interaction between transmembrane α-helices of subunit IV, Cyt b_6, and the minor subunits encoded by the *petL*, *petM*, and *petN* genes (Smith et al., 2004).

The impairment of the accumulation and function of Cyt b_6f in the FN68 mutant provides support for the latter suggestion. As the strain was grown in absolute darkness, it is extremely unlikely that the defect in complex accumulation is the result of photooxidative stress. In fact, the growth of FN68 is inhibited even upon illumination at very low photon flux densities (10 μE m^{-2} s^{-1}) in a nitrogen atmosphere supplemented with CO_2 but deprived of oxygen (Supplemental Fig. S9). However, given the very similar structure of the mitochondrial Cyt bc_1 complex (Crofts, 2004), the effect of the absence of the single β-carotene in Cyt b_6f appears to be quite dramatic, and it could be an indirect result of a more complex interplay between physiological processes affected by the absence of Cars in the mutant. In fact, the residual amount of complex accumulated appears to be, kinetically, as efficient as the wild type. As the assembly of Cyt b_6f in vivo is assisted by a complex folding machinery (Nakamoto et al., 2000), it is possible that β-carotene, rather than affecting the stability of the complex per se, is required at some stage during the assembly process.

The requirement of carotenes for the stabilization of folding is probably the reason for the lack of any significant accumulation of either the LHC complexes or the RC subunits of PSII. In these cases, not only are Cars much more abundant cofactors (three to four molecules per protein monomer) compared with the single molecule bound to Cyt b_6f, but they have been

shown to be fundamental for in vitro refolding of LHCs (Plumley and Schmidt 1987; Paulsen et al., 1993; Sandonà et al., 1998).

The only exception to the strict requirement for Cars to obtain a detectable level of accumulation of functional photosynthetic complexes is the RC of PSI, which is not only assembled but appears to operate with similar efficiency to the wild-type RC in the FN68 strain. These results are in agreement with the previous study of Bautista et al. (2005), who investigated *Synechocystis* sp. PCC 6803 mutants that contained only short-chain Cars. On the other hand, an increased sensitivity of PSI to photooxidative damage and a lower level of PSI accumulation have been reported in mutants of Arabidopsis with a lower β-carotene content with respect to xanthophylls compared with the wild type (Cazzaniga et al., 2012). However, the mutation analyzed by Cazzaniga et al. (2012) is far less dramatic than those investigated by Bautista et al. (2005) and in this study, where strains were grown in total darkness so that photoinhibition and photoprotection do not play a role in complex accumulation.

However, the variation in Chl levels observed among different phytoene synthase mutants including FN68 by McCarthy et al. (2004) suggests differences in the levels of accumulated PSI in different mutant backgrounds. This is confirmed by western-blot analysis of four mutants: FN68, w7, lts1-207, and lts-209, in which the PSI levels are estimated to be 25%, 15%, less than 1%, and less than 1%, respectively (Supplemental Fig. S4). Whether this reflects compensatory mutations in FN68 and w7, allowing increased accumulation of a PSI complex lacking carotenes (e.g. a mutation affecting a protease involved in PSI turnover), or additional mutations in the two lts1 strains (or their parent background), leading to increased PSI instability, is not clear and requires further genetic analysis. Nonetheless, the ability of FN68 to assemble a functional PSI RC despite the fact that the PsaA/PsaB heterodimer alone binds 22 β-carotene molecules, making it the second most abundant cofactor after Chl *a* (approximately 80 molecules per PsaA/PsaB heterodimer), is an intriguing observation. This suggests that the folding of PSI RC subunits in the thylakoid membrane is either substantially different from that of all other photosynthetic complexes or the folding of PSI RC polypeptides is sufficiently stable and the assembly of PSI can take place, to some extent, even in the absence of large amounts of cofactors. In this respect, it is interesting that the electron transfer chain of PSI maintains its functionality even in complexes in which the majority of cofactors have been extracted by treatment with organic solvent (Itoh et al., 2001). This points toward a particular thermodynamic stability of the secondary and ternary structures of the main constituents of the PSI RC compared with PSII and Cyt b_6f. Comparison of the crystallographic models of the PSI and PSII core complexes reveals a very similar arrangement of their transmembrane α-helices, which is the most abundant secondary motif. However, while the majority of pigments are bound to PsaA and PsaB in the PSI core, PSII chromophores are bound to four major subunits: D1, D2, CP43, and CP47 (Jordan et al., 2001; Ben-Shem et al., 2003; Guskov et al., 2009). This difference in the arrangement of RC subunits may be the basis for the superior stability of PSI RC, as all the transmembrane secondary structure elements are linked via the lumen and stroma-exposed loops of the PsaA and PsaB polypeptides, while weaker hydrophobic interactions play a larger role in the stabilization of the D1•D2•CP43•CP47 multimer that represents the bulk of the internal antenna and the catalytic core of PSII.

MATERIALS AND METHODS

Strains, Media, and Growth Conditions

The wild-type strain CC-1021 (mt+) and the Car-less strains FN68 (mt–) CC-2682, w-7 CC-2843, lts1-207 (mt+) CC-4113, and lts1-209 (mt+) CC-4115 were obtained from the *Chlamydomonas* Center (www.chlamy.org). The Δ*petD* (mt+) deletion strain and Fud7-P71, a double mutant with a Δ*psbA* deletion and reduced light-harvesting antenna (Byrdin et al., 2006), were from the Paris Culture Collection. All strains were maintained on Tris-acetate-phosphate medium under continuous illumination at a photon flux density of approximately 10 μE m^{-2} s^{-1} or, for the Car-less strains, in complete darkness. Cells were harvested by centrifugation at 1,500*g* for 5 min and immediately suspended in the appropriate medium for analysis.

Nuclear Transformation of FN68

The mutant was transformed using the glass beads method as described by Purton and Rochaix (1995) using a 4.4-kb PCR product containing the entire *PSY* gene amplified from wild-type genomic DNA using primers PSYg5′ and PSYg3′ (Supplemental Table S1). Transformant colonies were selected on Tris-acetate-phosphate plates under light of approximately 40 μE m^{-2} s^{-1} and scored for the presence of the wild-type *PSY* allele by PCR analysis using primers PSY5′ and PSY3′ (Supplemental Table S1) followed by digestion of the PCR product with *Sph*I.

Preparative and Analytical Techniques

Thylakoid Purification

Cells were harvested by centrifugation during the logarithmic growth phase and suspended in minimal growth medium to a concentration equivalent to 1 optical density at 680 nm. The thylakoids were purified by Yeda press (100 kg cm^{-2} fractionation as described previously; Santabarbara et al., 2007) with the following modifications: the harvesting buffer (0.6 M Suc, 100 mM Tricine-NaOH, pH 7.8, 20 mM NaCl, 10 mM $MgCl_2$, and 2 mM $CaCl_2$) also contained DNase I (100 μg mL^{-1}), phenylmethylsulfonyl fluoride (30 μg mL^{-1}), and bovine serum albumin (1%, w/v). The lysate was centrifuged at 250*g* for 5 min to remove unbroken cells and starch (all operations were performed either at 4°C or on ice and under darkness or very dim green light). The supernatant was then subjected to fractional centrifugation at 3,500*g* (10 min), 15,000*g* (10 min), and 35,000*g* (15 min). All pellets were washed in a buffer containing 0.1 M Suc, 20 mM Tricine-NaOH, pH 7.8, 10 mM NaCl, 5 mM $MgCl_2$, and 2 mM $CaCl_2$, centrifuged under the respective precipitation conditions, and finally suspended to a concentration equivalent to 500 μg mL^{-1} Chl *a* in 30 mM Tricine, pH 7.8, 10 mM NaCl, and 5 mM $MgCl_2$ for subsequent biochemical analysis. The light 35,000*g* fractions were used for comparative analysis of the wild type and FN68 (Fig. 2). The 3,500*g* thylakoid fraction was used for comparison of *C. reinhardtii* and spinach (*Spinacia oleracea*; Supplemental Figure S3).

SDS-PAGE and Western-Blot Analysis

Total protein extracts were prepared by growing cells to a density of approximately 4×10^6 mL^{-1}, centrifuging at 6,000*g* for 5 min, and resuspending

the pellet in 0.8 M Tris-HCl, pH 8.3, 0.2 M sorbitol, and 1% β-mercaptoethanol to a final concentration of approximately 8×10^7 mL^{-1}. Aliquots (50 μL) of boiled samples were separated by electrophoresis on a SDS-15% polyacrylamide gel and transferred to nitrocellulose membranes. Membranes were incubated with primary polyclonal antibodies at a dilution of 1:1,000. Membranes were incubated with a goat anti-rabbit secondary antibody at 1:5,000 dilution, conjugated to horseradish peroxidase, and enhanced chemiluminescence was used for autoradiographic detection (GE Healthcare).

In SDS-PAGE experiments aimed at resolving Cyt b_6f subunits, the samples were separated on a 12% to 18% gradient polyacrylamide gel containing 8 M urea. The gel was stained with 3,3′,5,5′-tetramethylbenzidine and revealed with hydrogen peroxide (Thomas et al., 1976).

Deriphat-PAGE

Deriphat-PAGE was carried out essentially as described by Peter et al. (1991) with the following modifications: a thin 4% acrylamide stacking gel was poured upon the 9% acrylamide running gel, and Deriphat concentration in the running buffer was reduced to 0.1% (w/v). For simultaneous analysis of wild-type and FN68 thylakoids, samples at equal total Chl concentration (10 μg) were solubilized using β-*n*-dodecyl maltoside at a final detergent:Chl weight ratio of 80:1. After 20 min of incubation on ice, samples were spun at 14,000 rpm for 30 min in a benchtop refrigerated centrifuge (4°C) to remove insolubilized material, and the supernatant was immediately applied to gels. Gels were run at a constant voltage of 50 V in the dark at 4°C.

EPR Spectroscopy

Continuous-Wave EPR

Continuous-wave EPR spectra were recorded on a JEOL RE1X spectrometer equipped with a cylindrical resonator that allows illumination of the sample in the spectrometer. The instrument is fitted with a cryostat (Oxford Instruments; ESR9) cooled with liquid helium, and the temperature is controlled with an ITC 5 unit (Oxford Instruments).

Time-Resolved EPR

Pulsed EPR kinetics was measured in a Bruker ESP580 spectrometer, operating at X-band (approximately 9.5 GHz), fitted with a dielectric resonator (Bruker model 1052 DLQ-H 8907) that has been described previously in detail (Santabarbara et al., 2006). The temporal resolution of the spectrometer is approximately 50 ns, limited by laser jitter and cavity ringing.

Samples

The samples at a Chl concentration equivalent to 2 mg mL^{-1} were placed in calibrated quartz tubes of 3 mm i.d. and incubated under an argon atmosphere for 30 min, on ice, prior to any chemical addiction. Photochemical reduction of $F_{A/B}$ and F_X was obtained as described previously (Santabarbara et al., 2005b, 2006).

Optical Spectroscopy

Fluorescence Emission Spectra

Fluorescence emission spectra were measured in a home-built apparatus: the excitation source consisted of a diode laser emitting at 465 nm, and the emission was collected by a CCD detector after dispersion through a spectrograph (Ocean Optics; HR4000) with a resolution of 1 nm. The fluorescence was excited, and the emission collected was from the surface of the sample through a fiber-optic system. The temperature was set by directly immersing the sample, at a concentration equivalent to 1 absorbance unit cm^{-1} at 680 nm and contained in a metal holder, into liquid nitrogen. The spectra were recorded after 10 min of incubation in the liquid nitrogen bath.

Absorption Spectra

Absorption spectra were measured in a home-built single-beam spectrometer, in the white light from a halogen lamp (Eurosep) shone on the sample, placed in a 1-cm path-length quartz cuvette, via a fiber-optic bundle, and the transmission was collected by a CCD detector (Ocean Optics; HR4000). The absorption spectrum was calculated from the recordings of the transmission. The optical resolution of the apparatus is 1 nm.

Time-Resolved Optical Spectroscopy

Time-resolved different absorption measurements in the submicrosecond time scale were performed employing a home-built pump-probe spectrophotometer that allows measurements to be performed in scattering biological material; the setup has been discussed previously in detail (Beal et al., 1999). In brief, the sample was excited at 700 nm, with a 7-ns pulse (full width at half maximum), obtained by pumping a dye laser (LDS 698) with a frequency doubled neodymium-doped yttrium aluminum garnet laser (Brilliant; Quantell). The intensity of the actinic pulse was set to a level ensuring single-turnover excitation of approximately 70% of the RCs. The kinetics were probed at different wavelength by 5-ns pulses (full width at half maximum) obtained by pumping an Optical Parametric Oscillator (Panther OPO; Continuum) with a frequency tripled neodymium-doped yttrium aluminum garnet laser (Surelite I; Continuum). The temporal resolution of the spectrometer is approximately 5 ns before instrument function deconvolution.

The cells were suspended at concentration equivalent to approximately 2 optical density cm^{-1} at 678 nm in a solution containing HEPES-NaOH buffer at pH 7 and 20% (w/v) Ficoll to avoid sedimentation of the sample during the measurements. The uncoupler carbonylcyanide *p*-trifluoromethoxy phenylhydrazone (10 μM) was added to the sample to avoid the establishment of long-lived ion fields across the thylakoid membrane.

Data Analysis

Global fittings of single-turnover decays associated with PSI and Cyt b_6f turnover were performed using a home-written routine operating in MatLab (Cambridge Soft) that minimizes the sum of squared residues by a combination of Simplex and Levenberg-Marquardt algorithms. The time decay of the ESE has been fitted with a sum of exponential functions as described previously (Santabarbara et al., 2005b).

Supplemental Data

The following materials are available in the online version of this article.

Supplemental Figure S1. HPLC analysis of the wild type and the FN68 mutant of *C. reinhardtii*.

Supplemental Figure S2. Restriction and PCR analysis of the FN68 mutation.

Supplemental Figure S3. Deriphat-PAGE and immunodecoration of native gels analysis.

Supplemental Figure S4. Quantification of PSI levels in FN68 by immunoblot analysis.

Supplemental Figure S5. Immunoblot analysis of FN68 transformed with the wild-type *PSY* gene.

Supplemental Figure S6. Kinetics of light-induced electron transfer reaction in PSI.

Supplemental Figure S7. Kinetics of light-induced electron transfer reaction at 265 and 100 K monitored by pulsed EPR spectroscopy.

Supplemental Figure S8. Continuous-wave EPR light-minus-dark difference spectra.

Supplemental Figure S9. Comparison of growth under different light intensities and atmosphere composition.

Supplemental Table S1. Oligonucleotide sequences from *PSY* used for PCR amplification.

ACKNOWLEDGMENTS

We acknowledge the early contribution made to this work by the late Mike Evans (University College London). We are grateful to Paul Fraser (Royal Holloway, University of London) for help with the HPLC analysis of FN68.

We thank Yves Pierre (Institut de Biologie Physicho Chimique) for his technical advice and Giuseppe Zucchelli (Istituto di Biofisica, Consiglio Nazionale delle Ricerche) for stimulating discussions. We thank Jean-David Rochaix (University of Geneva) for the PsaA, p11, and p15 antibodies and Peter Nixon (Imperial College London) for the D1 antibodies.

Received August 9, 2012; accepted November 14, 2012; published November 16, 2012.

LITERATURE CITED

Agalarov R, Brettel K (2003) Temperature dependence of biphasic forward electron transfer from the phylloquinone(s) A_1 in photosystem I: only the slower phase is activated. Biochim Biophys Acta **1604:** 7–12

Ali K, Santabarbara S, Heathcote P, Evans MCW, Purton S (2006) Bidirectional electron transfer in photosystem I: replacement of the symmetry-breaking tryptophan close to the PsaB-bound phylloquinone A_{1B} with a glycine residue alters the redox properties of A_{1B} and blocks forward electron transfer at cryogenic temperatures. Biochim Biophys Acta **1757:** 1623–1633

Bassi R, Pineau B, Dainese P, Marquardt J (1993) Carotenoid-binding proteins of photosystem II. Eur J Biochem **212:** 297–303

Bautista JA, Rappaport F, Guergova-Kuras M, Cohen RO, Golbeck JH, Wang JY, Béal D, Diner BA (2005) Biochemical and biophysical characterization of photosystem I from phytoene desaturase and zeta-carotene desaturase deletion mutants of *Synechocystis* sp. PCC 6803: evidence for PsaA- and PsaB-side electron transport in cyanobacteria. J Biol Chem **280:** 20030–20041

Beal D, Rappaport F, Joliot P (1999) A new high-sensitivity 10-ns time-resolution spectrophotometric technique adapted to *in vivo* analysis of the photosynthetic apparatus. Rev Sci Instrum **70:** 202–207

Ben-Shem A, Frolow F, Nelson N (2003) Crystal structure of plant photosystem I. Nature **426:** 630–635

Bolychevtseva YV, Rakhimberdieva MG, Karapetyan NV, Popov VI, Moskalendo AA, Kuznetsova NY (1995) The development of carotenoid-deficient membranes in plastids of barley seedlings treated with norflurazon. J Photochem Photobiol B **27:** 153–160

Butler WL (1978) Energy distribution in the photochemical apparatus of photosynthesis. Annu Rev Plant Physiol **29:** 345–378

Byrdin M, Santabarbara S, Gu F, Fairclough WV, Heathcote P, Redding K, Rappaport F (2006) Assignment of a kinetic component to electron transfer between iron-sulfur clusters F_X and $F_{A/B}$ of photosystem I. Biochim Biophys Acta **1757:** 1529–1538

Cazzaniga S, Li Z, Niyogi KK, Bassi R, Dall'Osto L (2012) The Arabidopsis *szl1* mutant reveals a critical role of β-carotene in photosystem I photoprotection. Plant Physiol **159:** 1745–1758

Choquet Y, Vallon O (2000) Synthesis, assembly and degradation of thylakoid membrane proteins. Biochimie **82:** 615–634

Claes H (1957) Biosynthese yon Carotinoiden bei Chlorella. 4. Die Carotinsynthese einer *Chlorella*-Mutante bei anaerober Belichtung. Z Naturforsch **12b:** 401–407

Crofts AR (2004) The cytochrome bc_1 complex: function in the context of structure. Annu Rev Physiol **66:** 689–733

Dashdorj N, Zhang H, Kim H, Yan J, Cramer WA, Savikhin S (2005) The single chlorophyll *a* molecule in the cytochrome b_6f complex: unusual optical properties protect the complex against singlet oxygen. Biophys J **88:** 4178–4187

Demmig-Adams B (1990) Carotenoids and photoprotection in plants: a role for the xanthophyll zeaxanthin. Biochim Biophys Acta **1020:** 1–24

Faludi-Dániel Á, Amesz J, Nagy AH (1970) P_{700} oxidation and energy transfer in normal maize and in carotenoid-deficient mutants. Biochim Biophys Acta **197:** 60–68

Faludi-Dániel Á, Fridvalszky L, Gyurján I (1968) Pigment composition and plastid structure in leaves of carotenoid mutant maize. Planta **78:** 184–195

Fiore A, Dall'Osto L, Cazzaniga S, Diretto G, Giuliano G, Bassi R (2012) A quadruple mutant of Arabidopsis reveals a β-carotene hydroxylation activity for LUT1/CYP97C1 and a regulatory role of xanthophylls on determination of the PSI/PSII ratio. BMC Plant Biol **12:** 50

Foster KW, Saranak J, Patel N, Zarilli G, Okabe M, Kline T, Nakanishi K (1984) A rhodopsin is the functional photoreceptor for phototaxis in the unicellular eukaryote *Chlamydomonas*. Nature **311:** 756–759

Frank HA, Cogdell R (1993) Photochemistry and function of carotenoids in photosynthesis. *In* A Young, G Britton, eds, Carotenoids in Photosynthesis. Chapman and Hall, London, pp 253–326

Giacometti G, Agostini G, Santabarbara S, Carbonera D (2007) ODMR spectroscopy of molecular functions of photosynthetic membrane proteins. Appl Magn Reson **31:** 179–191

Guergova-Kuras M, Boudreaux B, Joliot A, Joliot P, Redding KE (2001) Evidence for two active branches for electron transfer in photosystem I. Proc Natl Acad Sci USA **98:** 4437–4442

Guskov A, Kern J, Gabdulkhakov A, Broser M, Zouni A, Saenger W (2009) Cyanobacterial photosystem II at 2.9-A resolution and the role of quinones, lipids, channels and chloride. Nat Struct Mol Biol **16:** 334–342

Haehnel W (1984) Plastocyanin. Annu Rev Plant Physiol **35:** 659–693

Hideg E, Spetea C, Vass I (1994) Singlet oxygen and free radicals production during acceptor- and donor-side photoinhibition. Biochim Biophys Acta **1186:** 143–152

Hope AB (2000) Electron transfers amongst cytochrome f, plastocyanin and photosystem I: kinetics and mechanisms. Biochim Biophys Acta **1456:** 5–26

Horton P, Ruban AV, Walters RG (1996) Regulation of light harvesting in green plants. Annu Rev Plant Physiol Plant Mol Biol **47:** 655–684

Humbeck K, Romer S, Senger H (1989) Evidence for an essential role of carotenoids in the assembly of an active photosystem II. Planta **179:** 242–250

Ihalainen JA, Jensen PE, Haldrup A, van Stokkum IH, van Grondelle R, Scheller HV, Dekker JP (2002) Pigment organization and energy transfer dynamics in isolated photosystem I (PSI) complexes from *Arabidopsis thaliana* depleted of the PSI-G, PSI-K, PSI-L, or PSI-N subunit. Biophys J **83:** 2190–2201

Inwood W, Yoshihara C, Zalpuri R, Kim KS, Kustu S (2008) The ultrastructure of a *Chlamydomonas reinhardtii* mutant strain lacking phytoene synthase resembles that of a colorless alga. Mol Plant **1:** 925–937

Itoh S, Iwaki M, Ikegami I (2001) Modification of photosystem I reaction center by the extraction and exchange of chlorophylls and quinones. Biochim Biophys Acta **1507:** 115–138

Jennings R, Zucchelli G, Bassi R (1996) Antenna structure and energy transfer in higher plant photosystems. *In* J Mattay, ed, Topics in Current Chemistry, Vol. 177. Spinger-Verlag, Berlin, pp 147–181

Jordan P, Fromme P, Witt HT, Klukas O, Saenger W, Krauss N (2001) Three-dimensional structure of cyanobacterial photosystem I at 2.5 A resolution. Nature **411:** 909–917

Krieger-Liszkay A (2005) Singlet oxygen production in photosynthesis. J Exp Bot **56:** 337–346

Kurisu G, Zhang H, Smith JL, Cramer WA (2003) Structure of the cytochrome b_6f complex of oxygenic photosynthesis: tuning the cavity. Science **302:** 1009–1014

Li Y, van der Est A, Lucas MG, Ramesh VM, Gu F, Petrenko A, Lin S, Webber AN, Rappaport F, Redding K (2006) Directing electron transfer within photosystem I by breaking H-bonds in the cofactor branches. Proc Natl Acad Sci USA **103:** 2144–2149

McCarthy SS, Kobayashi MC, Niyogi KK (2004) White mutants of *Chlamydomonas reinhardtii* are defective in phytoene synthase. Genetics **168:** 1249–1257

Nakamoto SS, Hamel P, Merchant S (2000) Assembly of chloroplast cytochromes *b* and *c*. Biochimie **82:** 603–614

Nielsen VS, Mant A, Knoetzel J, Møller BL, Robinson C (1994) Import of barley photosystem I subunit N into the thylakoid lumen is mediated by a bipartite presequence lacking an intermediate processing site: role of the delta pH in translocation across the thylakoid membrane. J Biol Chem **269:** 3762–3766

Niyogi KK (1999) Photoprotection revisited: genetic and molecular approaches. Annu Rev Plant Physiol Plant Mol Biol **50:** 333–359

Paulsen H, Finkenzeller B, Kühlein N (1993) Pigments induce folding of light-harvesting chlorophyll *a*/*b*-binding protein. Eur J Biochem **215:** 809–816

Peter GF, Takeuchi T, Thornber JP (1991) Solubilization and two-dimensional electrophoretic procedures for studying the organization and composition of photosynthetic membrane polypeptides. Methods **3:** 115–124

Peterman EJ, Wenk SO, Pullerits T, Pâlsson LO, van Grondelle R, Dekker JP, Rögner M, van Amerongen H (1998) Fluorescence and absorption spectroscopy of the weakly fluorescent chlorophyll *a* in cytochrome b_6f of *Synechocystis PCC6803*. Biophys J **75:** 389–398

Plumley FG, Schmidt GW (1987) Reconstitution of Chl *a*/*b* light-harvesting complexes: xanthophyll-dependent reconstitution and energy transfer. Proc Natl Acad Sci USA **84:** 145–150

Purton S, Rochaix J-D (1995) Characterisation of the *ARG7* gene of *Chlamydomonas reinhardtii* and its application to nuclear transformation. Eur J Phycol **30:** 141–148

Rijgersberg CP, Amesz J (1980) Fluorescence and energy transfer in phycobiliprotein-containing algae at low temperature. Biochim Biophys Acta **593:** 261–271

Sandonà D, Croce R, Pagano A, Crimi M, Bassi R (1998) Higher plants light harvesting proteins: structure and function as revealed by mutation analysis of either protein or chromophore moieties. Biochim Biophys Acta **1365:** 207–214

Santabarbara S, Agostini G, Casazza AP, Syme CD, Heathcote P, Böhles F, Evans MC, Jennings RC, Carbonera D (2007) Chlorophyll triplet states associated with photosystem I and photosystem II in thylakoids of the green alga *Chlamydomonas reinhardtii*. Biochim Biophys Acta **1767:** 88–105

Santabarbara S, Galuppini L, Casazza AP (2010a) Bidirectional electron transfer in the reaction centre of photosystem I. J Integr Plant Biol **52:** 735–749

Santabarbara S, Heathcote P, Evans MCW (2005a) Modelling of the electron transfer reactions in photosystem I by electron tunnelling theory: the phylloquinones bound to the PsaA and the PsaB reaction centre subunits of PSI are almost isoenergetic to the iron-sulfur cluster F(X). Biochim Biophys Acta **1708:** 283–310

Santabarbara S, Jasaitis A, Byrdin M, Gu F, Rappaport F, Redding K (2008) Additive effect of mutations affecting the rate of phylloquinone reoxidation and directionality of electron transfer within photosystem I. Photochem Photobiol **84:** 1381–1387

Santabarbara S, Kuprov I, Fairclough WV, Purton S, Hore PJ, Heathcote P, Evans MCW (2005b) Bidirectional electron transfer in photosystem I: determination of two distances between P_{700}^{+} and A_1^{-} in spin-correlated radical pairs. Biochemistry **44:** 2119–2128

Santabarbara S, Kuprov I, Hore PJ, Casal A, Heathcote P, Evans MCW (2006) Analysis of the spin-polarized electron spin echo of the $[P_{700}^{+} A_1^{-}]$ radical pair of photosystem I indicates that both reaction center subunits are competent in electron transfer in cyanobacteria, green algae, and higher plants. Biochemistry **45:** 7389–7403

Santabarbara S, Kuprov I, Poluektov O, Casal A, Russell CA, Purton S, Evans MCW (2010b) Directionality of electron-transfer reactions in photosystem I of prokaryotes: universality of the bidirectional electron-transfer model. J Phys Chem B **114:** 15158–15171

Santabarbara S, Redding KE, Rappaport F (2009) Temperature dependence of the reduction of P_{700}^{+} by tightly bound plastocyanin *in vivo*. Biochemistry **48:** 10457–10466

Santabarbara S, Reifschneider K, Jasaitis A, Gu F, Agostini G, Carbonera D, Rappaport F, Redding KE (2010c) Interquinone electron transfer in photosystem I as evidenced by altering the hydrogen bond strength to the phylloquinone(s). J Phys Chem B **114:** 9300–9312

Schlodder E, Falkenberg K, Gergeleit M, Brettel K (1998) Temperature dependence of forward and reverse electron transfer from A_1^{-}, the reduced secondary electron acceptor in photosystem I. Biochemistry **37:** 9466–9476

Siefermann-Harms D (1985) Carotenoids in photosynthesis. I. Location in photosynthetic membranes and light-harvesting function. Biochim Biophys Acta **811:** 325–355

Smith JL, Zhang H, Yan J, Kurisu G, Cramer WA (2004) Cytochrome *bc* complexes: a common core of structure and function surrounded by diversity in the outlying provinces. Curr Opin Struct Biol **14:** 432–439

Srinivasan N, Golbeck JH (2009) Protein-cofactor interactions in bioenergetic complexes: the role of the A1A and A1B phylloquinones in photosystem I. Biochim Biophys Acta **1787:** 1057–1088

Srinivasan N, Santabarbara S, Rappaport F, Carbonera D, Redding K, van der Est A, Golbeck JH (2011) Alteration of the H-bond to the A_{1A} phylloquinone in photosystem I: influence on the kinetics and energetics of electron transfer. J Phys Chem B **115:** 1751–1759

Stroebel D, Choquet Y, Popot J-L, Picot D (2003) An atypical haem in the cytochrome b_6f complex. Nature **426:** 413–418

Thomas PE, Ryan D, Levin W (1976) An improved staining procedure for the detection of the peroxidase activity of cytochrome P-450 on sodium dodecyl sulfate polyacrylamide gels. Anal Biochem **75:** 168–176

Trebst A, Depka B (1997) Role of carotene in the rapid turnover and assembly of photosystem II in *Chlamydomonas reinhardtii*. FEBS Lett **400:** 359–362

Umena Y, Kawakami K, Shen JR, Kamiya N (2011) Crystal structure of oxygen-evolving photosystem II at a resolution of 1.9 Å. Nature **473:** 55–60

Young A, Britton G (1993) Carotenoids in Photosynthesis. Chapman and Hall, London